Taking the Pulse of Our Ocean World

David R. Dall'Osto

Address:
Applied Physics Laboratory
University of Washington
1013 NE 40th Street
Seattle, Washington 98105
USA

Email:
dallosto@uw.edu

The lost* San Juan *submarine was triangulated by the precision CTBT hydroacoustic network, which has great potential for ocean science.

Twenty years ago, the United Nations decided to collectively build what is, in essence, a stethoscope to continuously monitor the oceans in the world for the early detection of the most serious danger to world peace and survival, nuclear explosions (see ctbto.org). The impetus for creating this US$5 billion global network was to enforce compliance with the Comprehensive Nuclear Test Ban Treaty (CTBT). This network is designed to locate all types of nuclear tests (in the air, on land, underground, and underwater) to within an area less than 1,000 km^2. The CTBT Organization (CTBTO) coordinates, maintains, and analyzes the data from these International Monitoring System (IMS) hydroacoustic stations along with the data from land-based infrasonic, seismic, and radionuclide detectors.

Six remote locations around the globe were chosen for detecting underwater detonations. Each location was instrumented with a set of sensitive hydrophones suspended deep within the ocean, at depths that would crush a submarine hull. The design of these moorings was optimized to measure sound propagating over great distances (see **Figure 1** for the anatomy of an IMS hydroacoustic station). The record of ocean sound compiled as a consequence of the mission of the IMS network is a resource of vast potential for researchers in many fields, both for forward-looking and for historical scientific analysis.

Figure 1. *"Anatomy" of an International Monitoring System (IMS) hydroacoustic station. Hydrophones are moored close to the axis of the SOFAR channel formed by the sound speed profile (**left**). Each station is composed of two triplets, one located on either side of the island housing the shore facility that telecommunicates the data (except station HA01 that has only 1 triplet; **right**). See text for details. Adapted from a figure courtesy of CTBTO.org.*

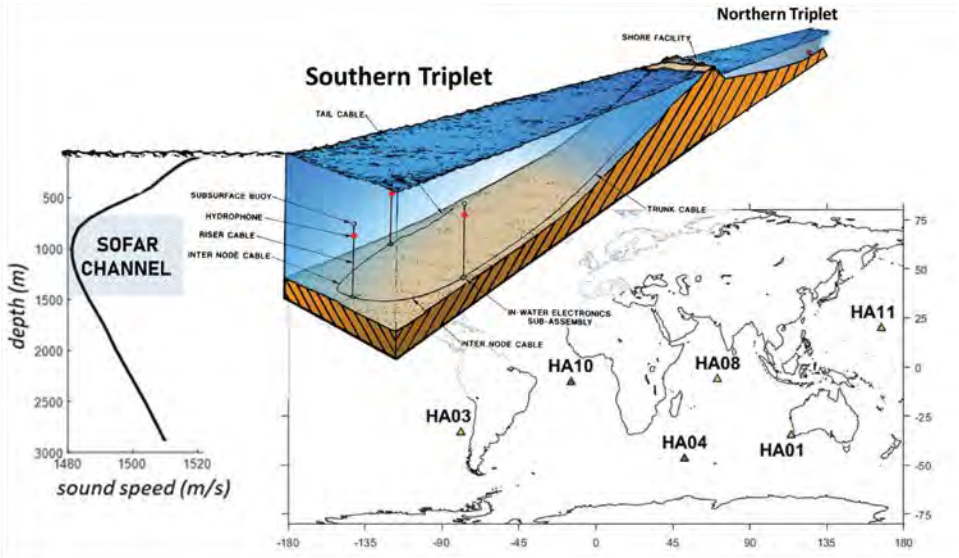

https://doi.org/10.1121/AT.2019.15.4.20

A recent example of the IMS hydroacoustic network providing a service beyond its original mission purpose of detecting nuclear detonations was its role in finding the lost Argentine submarine ARA *San Juan*. Triangulation of the intense sound generated by the *San Juan*, presumably from the rapid collapse of its hull when it exceeded its crush depth, was the crucial piece of evidence that led to its discovery, 920 meters below the ocean's surface. Although the sinking of the ARA *San Juan* was a tragedy, the methods used to find it provide an example and source of future opportunity. Hydroacoustic triangulation of the *San Juan* was possible due to the precision of the IMS recordings and a reliable estimate of the ocean climate, an example being the World Ocean Atlas (see www.nodc.noaa.gov).

Quoting the study by the National Research Council (2011, p. 108) on climate change-related technical issues impacting naval operations, "The U.S. Navy and other world navies have invested large sums to acquire field measurements of temperature and salinity, as well as bathymetry, to produce climatological "atlases"... [and while] it would be comforting to assume that climate-induced ocean changes will be slow, and that the impact on current data atlases will be minimal... not enough is known about climate change to be assured of these assumptions. Although it was possible to triangulate the *San Juan* to within a few kilometers with these atlases, the inaccuracy ultimately boils down to an ill-constrained state estimate of the ocean climate. In fact, a correction to the errors for a known source location provides a constraint for estimating the climate of the ocean, a process known as acoustic thermometry (or tomography). As shown here, the impulse signal from the *San Juan* is imprinted with a signature of the oceanography it propagated through. Further review and analysis of the IMS record of ocean sound may be an important sentinel of the extent and rate of climate change and global warming.

Acoustic tomography is one example as to why ocean sound has been defined as an essential ocean variable (see goosocean.org). Ocean sound serves as an indicator pertinent to physical, chemical, and biological oceanographic processes. The remote static measurements of the IMS stations provide a natural laboratory and historical data bank to study low-frequency ocean noise (Bradley and Nichols, 2015) and infer temperature (Sabra et al., 2016). The most intense sounds in the hydroacoustic recordings are generated by catastrophic events (underwater earthquakes, landslides, and volcanic eruptions), including ones that were devastating to humans such as the Sumatra-Andaman earthquake of 2004. Analysis of that event and its potential for early warning tsunami detection were, in part, a motivating factor to put IMS recordings of ocean sound into the public domain.

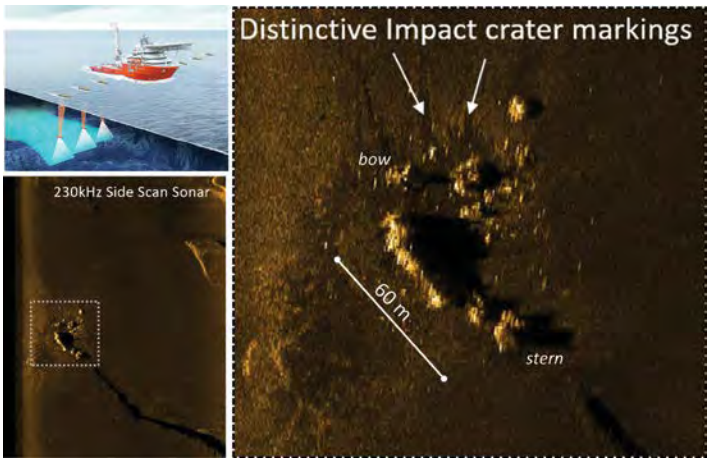

Figure 2. Left top: *in 60 days, 5 Hugin autonomous underwater vehicles surveyed 21,000 km² of the seafloor with their side-scan sonars.* ***Left bottom:*** *230-kHz backscatter image in which the ARA* San Juan *was clearly identified, resting on a small ridge in a ravine 920 m deep.* ***Right:*** *an enlargement of the* San Juan *debris field. Image courtesy of Ocean Infinity.*

The Search for the ARA *San Juan*

"On the night of 14 November 2017, facing rough seas, the commanding officer reported a water entry (apparently through the snorkel) that had caused a short circuit in the forward battery compartment. A fire followed, but it was controlled by the crew. The *San Juan* then was ordered to change course and return directly to her home port, Mar del Plata, Argentina" (Villán, 2019, p. 1393). The last transmission received from the *San Juan* was at 1019 Coordinated Universal Time (UTC) on November 15, 2017. Two and a half hours later, the submarine exceeded its maximum depth rating as it sank to the bottom of the ocean and was crushed by extreme water pressure. An intense sonic impulse was generated by the compression phase of the hull collapse, lasting roughly 35 milliseconds based on acoustic and forensic analyses of the USS *Scorpion* submarine, which, too, after suffering a battery fire, lost buoyancy and sank beyond its crush depth in 1968 (Bruce Rule, personal communication, 2018).

The sound generated by the catastrophic event of the sinking of the *San Juan* was detected by 2 IMS hydroacoustic stations, one over 6,000 km away in the mid-Atlantic Ocean and the other 8,000 km away in the Southern Indian Ocean. CTBTO

scientists analyzed the acoustic anomaly and reported the event to the search and rescue (SAR) operation, which commenced with great international support. Two weeks later, the SAR operation had turned into a recovery mission. This mission ended exactly one year and a day after the sinking, when the *San Juan* was identified in a side-scan sonar image (see **Figure 2**). The acoustic signals pinpointed the location of the ARA *San Juan* to within 1,000th of the total propagation distance, an impressive result that demonstrates the capability of the CTBT network to enforce the nuclear test ban treaty.

So how exactly was the location of the *San Juan* determined from the hydroacoustic recordings? In part, the triplet design of the IMS stations (see **Figure 1**) measures the direction of arrival (DOA) of incoming sound energy. This information helps to associate signals that, due to the geographic dependence of dispersion, appear very different to the same event. A general area from the two station detections is established by the intersection of the geodesics along the DOA, but real precision in location comes from triangulation (which requires at least three detections). With this in mind, let us examine the method used to triangulate a sound impulse of unknown origin.

Triangulation of Unknown Acoustic Events

To introduce acoustic triangulation, we use a familiar example, ranging an approaching thunderstorm by counting seconds between a flash of lightning and the sound of a thunderclap. For this exercise, assume the simplest of environments, free space, a uniform environment with no boundaries and propagation speed equal to the speed of sound (c; 340 m/s in air). The acoustic wave front of an impulse (its shock wave) expands as a spherical surface centered at the origin of the source, with the radius (R) equal to the speed of sound times the time-of-flight (T). For thunderstorm ranging, the T is the time between the flash and the sound. Asserting that the sound origin and listeners all lay within the same plane, the projection of the spherical surface of the wave front on a two-dimensional map is an expanding circle, also with radius R (see **Figure 3**).

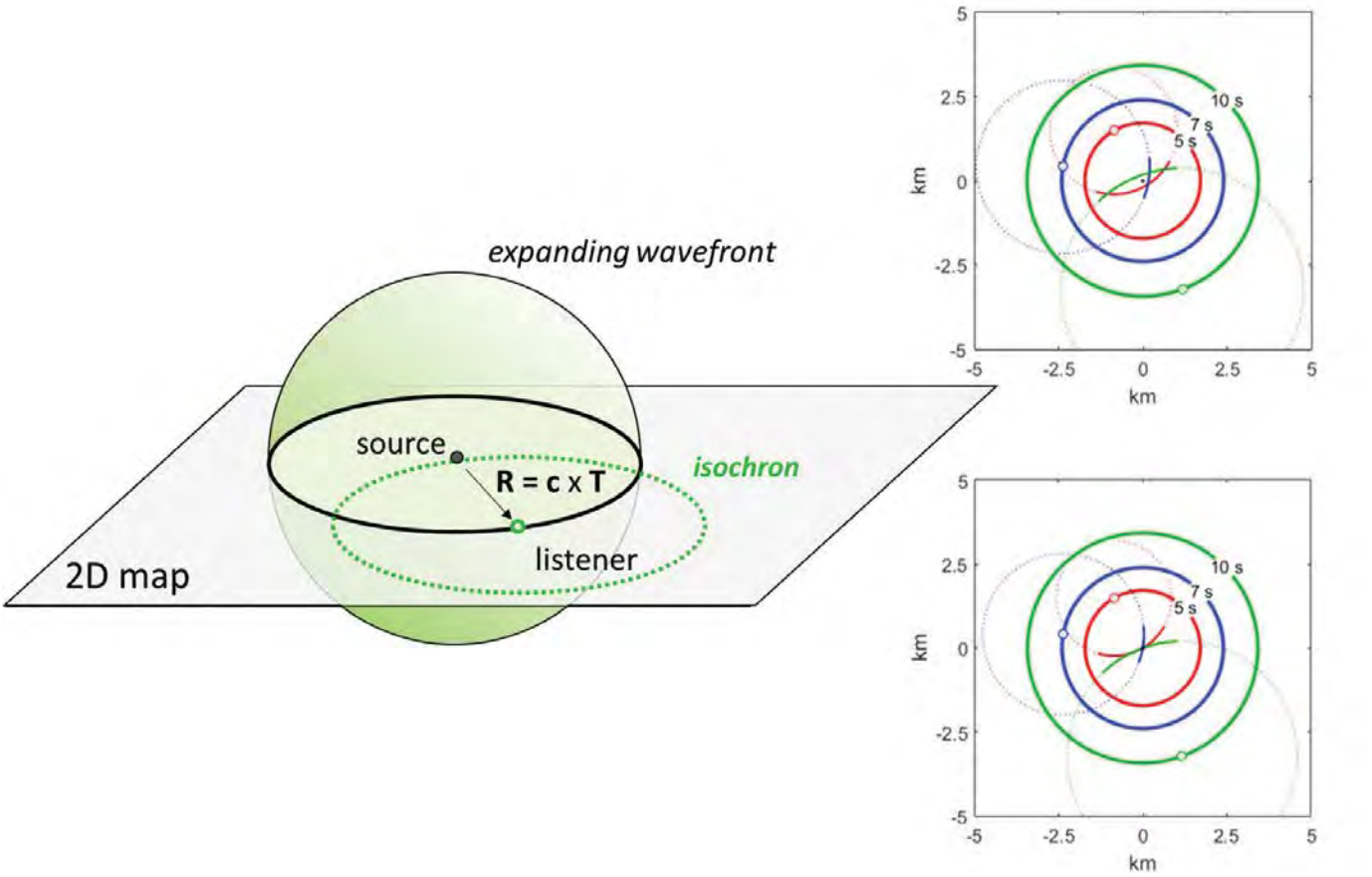

Figure 3. Left: *3-D wave front, projected onto the 2-D plane of the source and listener.* ***Right:*** *triangulation via 3 listeners at a candidate event time 0.5 seconds earlier than the actual time (**top**) or with a candidate event time equal to the actual time (**bottom**).*

In triangulation, we invoke a powerful tool, the principal of reciprocity that states that sound propagation from a source to a listener is identical to the backpropagation from the listener to the source. As such, the time it takes for an impulse of sound (a wave front) to reach a listener is equal to the time that it would take sound from the listener to propagate back to the origin. From this, we can form an isochron, which is a surface centered at the listener that connects points at which something occurs at the same time. Points on the isochron surface are all possible source origins. Thus, a single "listener" cannot determine exactly where the sound origin is located, being unable to distinguish where it lay exactly on its isochron. If a second listener saw and heard that event, likely with a different T based on its relative position to the source, its isochron and the intersection with the first identify the sound origin. Except when the listeners and source are in-line, the circular isochrons intersect at two points. A third listener reduces ambiguity.

Triangulation is the process of finding the precise location at the intersection of multiple isochrons. Now, if the listeners did not see the flash of lightning, then they do not know the T beforehand. A guess, or candidate event time, must be made from which to subtract the arrival time (when the thunder was heard), establishing a respective T to each listener. **Figure 3** shows two examples of triangulation with three listeners based on two candidate event times. One candidate time is one-half of a second before the actual event time (**Figure 3**, ***top right***); the three isochrons all intersect at different points surrounding the origin of sound. It is the third isochron that creates a solvable system of equations decoupled in range and time, such that all three isochron intersect only at one candidate event time. With the proper propagation speed, this equals the actual time (**Figure 3**, ***bottom right***) and all three isochrons intersect at the sound origin. So, as a rule, three arrivals are needed to triangulate an unknown event.

Nuances of Hydroacoustic Triangulation

Sound speed in the ocean is not uniform in all directions, and although the free-space example was useful in thunderstorm ranging, it is far too simplistic to model ocean propagation. Sound speed is faster in warmer water and in deeper water due to hydrostatic pressure. Long-range acoustic propagation in the ocean is possible due to trapping by upward and downward refraction (or reflection) processes. Consecutive surface reflections and refraction fold and distort a spherically expanding wave front, elongating the duration of an impulse through a process called geometric dispersion. Geometric dispersion of the *San Juan* signal, presumed to be an impulse with duration on the order of <1 second, caused an increase in the signal duration to well over 30 seconds.

To examine the dispersion and general signal timing (kinematics), we can form acoustic rays, which are lines drawn normal to an expanding wave front. Rays represent the trajectory of sound traveling at the local speed of sound and integrating the reciprocal of sound speed along the ray gives the T to the ray terminus. Rays are defined by a launch angle (Θ), the starting angle of the ray trajectory. Asserting that a wave front spherically expands in the immediate vicinity of the source, meaningful rays can be launched upward, downward, or horizontal. The largest $\pm\Theta$ that avoids a surface (and/or bottom) reflection is the limiting ray.

Figure 4 shows a group of rays, or ray fan, spanning the limiting ray for two environments that are representative of the ocean structure encountered by the propagating *San Juan* signal. **Figure 4**, ***left top***, shows a polar environment idealized as a 17 m/s increase in sound speed per kilometer of depth; **Figure 4**, ***left bottom***, is representative of a midlatitude ocean, which, in addition to the increase in sound speed with depth, has a warm layer in the upper ocean and thus has a higher speed near the surface and a minimum close to 1,000 meters deep. The rays in these two environments follow different

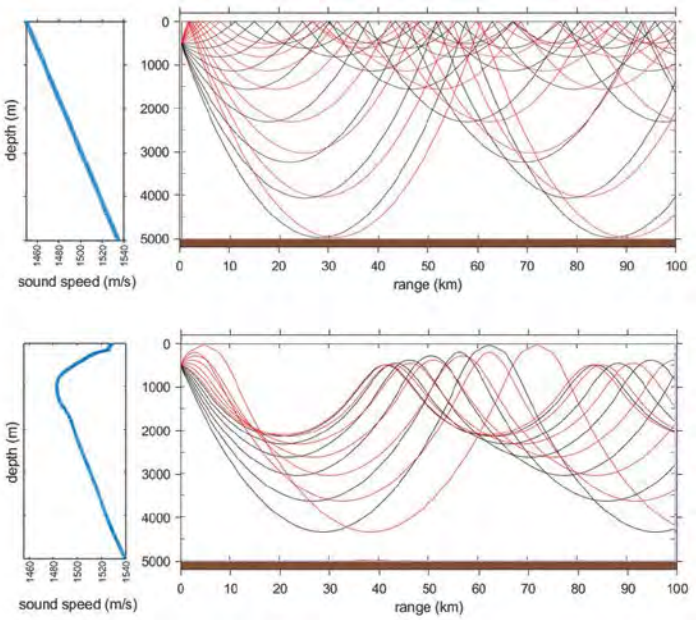

Figure 4. Left: *depth-dependent sound speed profile for a polar profile (**top**) and a midlatitude profile (**bottom**). **Right:** acoustic ray fans for the two environments spanning the limiting angle: **red lines**, rays launched upward; **black lines**, rays launched downward.*

paths, and from this, we can expect that dispersion depends on the oceanography. One consequence of refraction are shadow zones, areas where rays do not pass and sound from the source is not heard.

In comparing the two environments, note how the midlatitude sound speed profile adds a component of downward refraction, further isolating the signal from sea-surface reflections. The IMS station hydrophones are moored at an optimal depth, both to minimize the effect of shadow zones and to maximize the reception of all paths. In the midlatitudes, the optimal depth occurs at the axis of the well-known sound duct (see **Figure 1**), the SOFAR channel, named after the 1940s SOund Fixing And Ranging triangulation system that was developed to rescue downed pilots. The SOFAR system triangulated impulsive signals from bombs or "implosion discs" deployed by downed pilots. The discs were set with a fuse to detonate at a prescribed depth, geographically chosen to be at the SOFAR axis, to maximize the chance of detections by at least three search and rescue monitoring stations (Bureau of Naval Personnel, 1953, p. 282).

In the deep ocean, rays with steep angles sample higher sound speeds, and although having longer paths, this deep diving portion of the wave front actually travels faster than the part initially traveling horizontally. Thus, as a signal propagates further and further away from its source, its wave front elongates, with the steep rays arriving first, followed eventually by the horizontal rays. An important observation (see **Figure 4**) is that rays at $\pm\Theta$ follow the same path, albeit with a spatial offset near the source corresponding to the initial surface reflection (or refraction) of the positive angles. This pair of up-and-down rays arrive at the same time, and depending on frequency (f), the folded wave front here may reinforce through constructive interference. These pairs of up-and-down going rays define the propagating modes, and through a ray-mode analogy, these specific frequency-dependent ray launch angles correspond to a mode angle. As modes may not be familiar, let us take a minute to discuss what an oceanic mode is, and afterward, the advantage of decomposing a signal, like that from the *San Juan*, into a discrete set of modal arrivals should be clear.

Oceanic Mode Propagation

To introduce modes, let us consider vibration of a guitar string (see **Figure 5**). Modes are standing waves, waves not propagating in the direction in which they are defined. (e.g., along the guitar string), but are a description of the amplitude of the oscillations. When a guitar string is plucked, it is very clear that the motion resembles a half sine wave, pinned at one end by the nut (**Figure 5**, ***top***) and the bridge at the other end (**Figure 5**, ***bottom***). This is mode-1, the most basic motion that satisfies the boundary condition that the string does not move at the bridge or nut. Mode-2 may not be obvious; it resembles a full sine wave with a node or zero point of motion at the midpoint of the string (the 12th fret). To excite mode-2 and not mode-1, one can (with some practice) excite "the harmonic" by placing a finger lightly on the string at the half-way point and pluck the string on either side with the other hand. The light finger touch suppresses motion at the midpoint, letting only those modes with a node there vibrate (mode-2).

Mode shapes of a sound duct are also sinusoid-like. The mode shape describes the amplitude of a standing wave in depth, which propagates down the duct (away from the source) at its propagation speed. Revisiting the ray mode analogy, a pair of rays are associated with each mode. The plus or minus ray launch angles establish the mode angle, mathematically representing the trajectory of two interfering up-and-down-going plane waves (wave fronts with no curvature) that form the mode. The trajectory of the analogous rays sweep through the vertical (depth) extent of the mode shape. Also, the average propagation speed of the ray over one "ray cycle" (or the distance before the ray trajectory repeats) is equal to the mode propagation speed.

For the modes in a deep-ocean duct, mode angles are between the horizontal and the limiting rays. In shallower oceans, the physics of bottom reflection must be considered, and the mode angle is limited to within the critical angle, the shallow angle where total reflection occurs, and no energy is

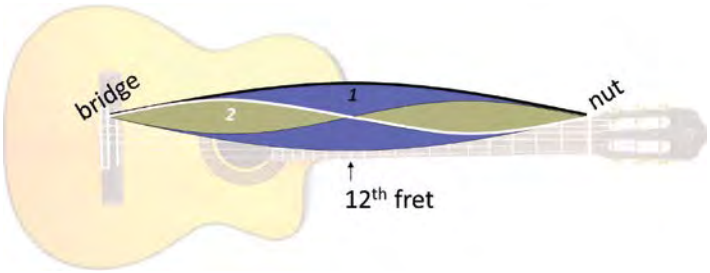

Figure 5. *Mode-1 (**black**) and mode-2 (**white**) of guitar string. The shaded areas represent the area swept out by the string vibration of mode-1 or mode-2 (displacement is exaggerated). Note the node, or stationary point of mode-2, at the 12th fret. See animation at acousticstoday.org/dallosto-multimedia.*

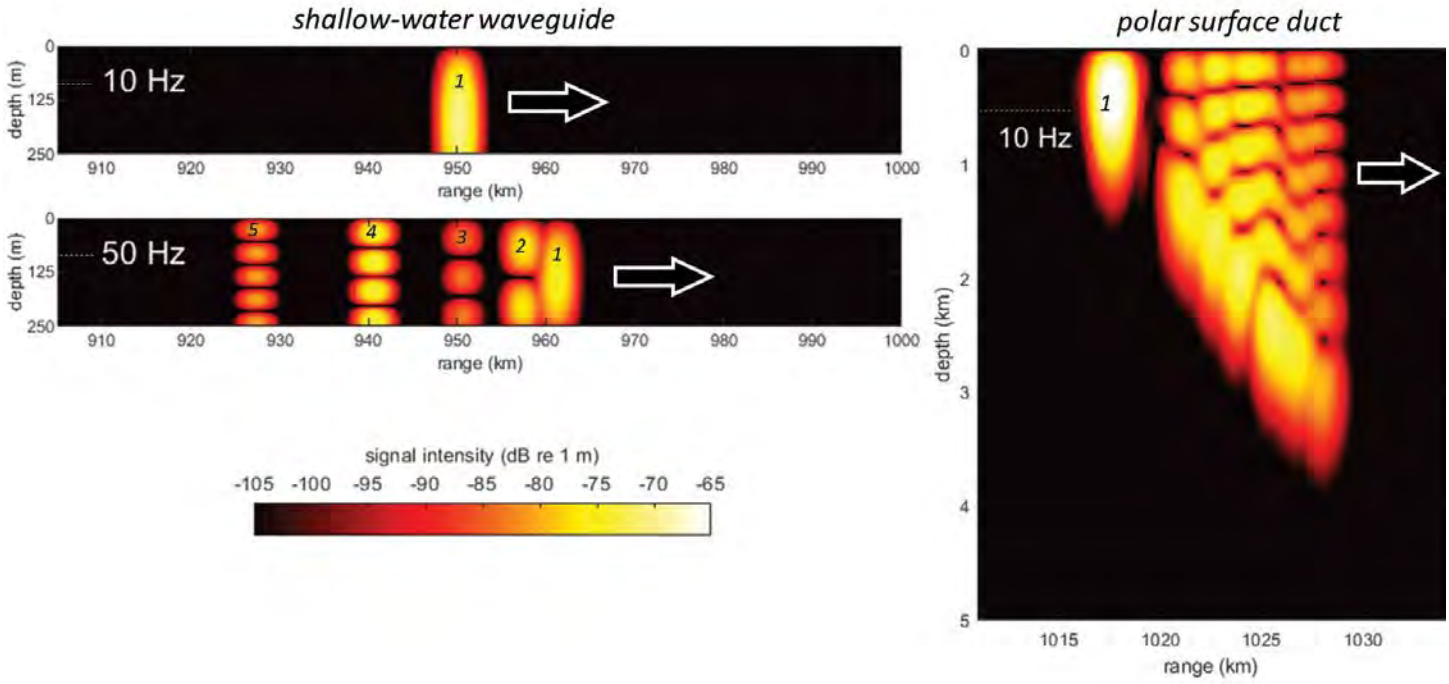

Figure 6. *Propagation of a half-second-duration impulse in a 250-meter deep ocean representative of the continental shelf at 10 Hz (**left top**) and 50 Hz (**left bottom**) and in a deep polar ocean (see **Figure 3**) at 10 Hz (**right**). **Arrows**, propagation direction; **numbers**, modal arrivals.*

transmitted through the boundary. The mode angle increases with mode number, as do the number of nodes. As such, each mode has a distinct propagation speed, and after propagating long distances, the dispersed signal separates into distinct modal arrivals.

Figure 6 shows the propagation of a half-second-long impulse out at 1,000 km in 2 environments, representative of the continental shelf and a deep polar ocean (as in **Figure 4**). At 10 Hz, only 1 mode (mode-1) exists or "fits" on the shallow continental shelf. Note that number of modes that can fit depends on the frequency, water depth and temperature, and composition of the seafloor sediments (Frisk, 1994, p. 151). At 50 Hz, 5 propagating modes exist on the continental shelf. Additional modes enter at the critical or limiting ray angle, shifting the mode-1 angle closer to the horizontal.

In the shallow-ocean propagation in **Figure 6**, ***left***, the mode-1 arrives first, followed sequentially by the higher order modes. This order is explained by steeper mode angles lengthening the analogous ray path through multiple reflections. In the deep polar ocean, the sequence of mode arrivals is reversed from the shelf propagation. This reversal is due to steeper analogous rays traveling at the faster sound speed of the deep ocean. **Figure 6**, ***right***, shows propagation in the polar environment at 10 Hz, where 8 modes exist now and mode-8 arrives well before mode-1. Inspecting the polar propagation in **Figure 6** in more detail, there is also a gap between the mode-1 arrival and what appears to be a mode-3, as if mode-2 is missing. In this illustrative example, the source is at a node of mode-2 and thus mode-2 was never excited. Because mode-1 does not have a node, its arrival should always be identifiable in a signal; it is special.

The travel time of a particular mode is the integrated reciprocal of its propagation speed along its path and is both frequency and geographically dependent. The time-frequency characteristics of the *San Juan* impulse show a clear geographic dependence to dispersion. Comparing the signals in **Figure 7**, the one that propagated through polar waters hardly resembles the signal that propagated through the SOFAR channel (see **Figure 8** for a reference map of the propagation paths). In these spectrograms of the signal, mode-1 corresponds to the peak energy arrival (**Figure 7**, ***red***). The mode-1 arrival time in the mid-Atlantic recording (**Figure 7**, ***left***) is essentially frequency independent, as evidenced at the vertical line at 14:59:18. The mode-1 arrival time at the polar station is frequency dependent, seen as a linear slope from 15:19:35 at 3 Hz to 15:20:00 at 10 Hz. This slope is due to the mode-1 angle shifting closer to the horizontal (having

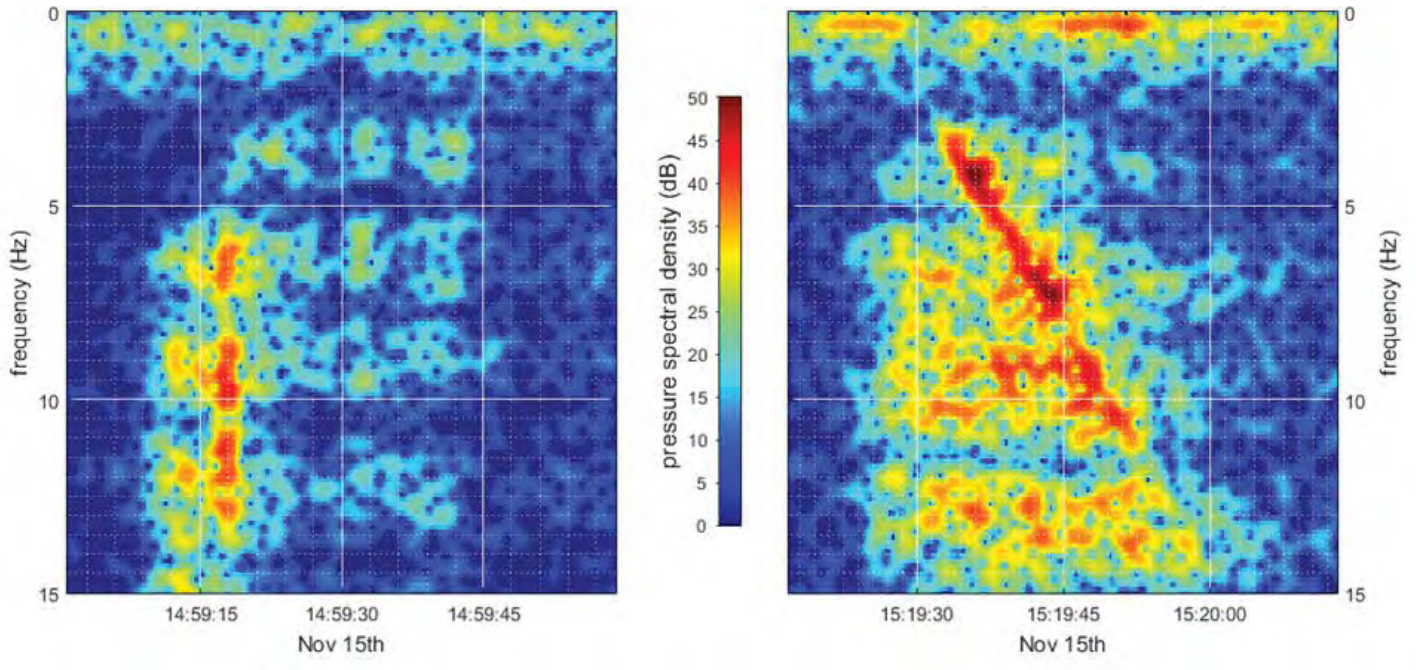

Figure 7. *Time-frequency spectrograms of the 2017* San Juan *impulse measured at the mid-Atlantic station HA10, having propagated within the SOFAR channel (**left**), and at the southern Indian Ocean station HA04, having propagated through a polar environment (**right**).*

a slower propagation speed in the polar profile) as the frequency increases.

A comparison of the two signals makes clear the task at hand, which is accurately "picking" signal features and associating them to the correct propagation speed. Although multiple isochrons can be formed from the modal arrivals, triangulation really benefits from forming isochrons along different propagation paths (triangulation does not work when three listeners are at the same location). In triangulation of the *San Juan* with the two hydroacoustic stations, additional isochrons are formed from three-dimensional (3-D) arrivals that had propagated off the geodesic or shortest path.

Triangulating the ARA *San Juan*

At low frequencies, relevant to the CTBT network, variability in modal propagation speed depends primarily on the ocean bottom topography (bathymetry). As sound propagates near sea mounts, islands, or the continental shelf, interaction with the bottom steepens the angle of a mode. This steepening causes sound waves to turn or refract away from (but depending on oceanography sometime toward) bathymetric features (Munk and Zachariasen, 1991). As sound energy travels up the slope and approaches the apex (the depth where a mode no longer fits), it is translating along the slope analogous to a ball rolling up an inclined plane at an angle. The sound turns and then travels back down, out toward deeper water.

Bottom topography in the vicinity of the *San Juan* was conducive to bathymetric refraction, and a plethora of 3-D arrivals were received at the mid-Atlantic IMS station (HA10). One of these arrivals had considerable amplitude and corresponded to energy refracted by the continental slope. The propagating wave front of mode-1 gets folded by the refraction process (its apex occurs at a depth of ~200 m), and from this, an additional isochron is formed based on that path (Dall'Osto, 2019).

Considering these two mode-1 arrivals and the arrival along the southern path, we have the three necessary for triangulation. After computing propagation paths and tabulating the propagation speed along each path, isochrons are formed perpendicular to the propagation paths. The isochron intersection occurs within a few kilometers of the actual location (see **Figure 8**). What remains that causes the error or mismatch between the actual and triangulated locations are inaccuracies in picking out the timing of the mode arrival and an ill-constrained estimate of the climate state of the ocean. Through inclusion of additional arrivals, these errors can be resolved.

Tomography Potential on the Comprehensive Nuclear Test Ban Treaty Network

Although it is clear that the accuracy with which we know the climate state of the ocean is needed for triangulation, knowing the ocean climate is of great importance to human civilization. As the oceans of the Earth are the primary heat sink on the planet, thermal expansion of the seawater from increasing temperature is a major factor driving rising sea levels. The methods currently being utilized to determine ocean temperature are based on direct sampling from oceanographic profilers or indirect measurements from space-based sensors. Oceanographic profilers represent point measurements of temperature (and other essential ocean variables) with respect to depth and include moored or ship-based measurements systems and autonomous systems such as sea gliders or drifting Argo floats (see argo.ucsd.edu). These space-based sensors, like those on the Geostationary Operational Environmental Satellites (GOES), provide two important parameters for ocean temperature and climate estimation and sea surface- and depth-averaged ocean temperature (as inferred by thermal expansion). In theory, with a dense enough network, this might be sufficient. However, maintaining global coverage with these types of systems requires ongoing deployment operations, and some areas, specifically near the poles, are extremely difficult to sample due to currents and sea-ice coverage.

This deficiency in sampling the ocean climate can be fulfilled with acoustic ocean tomography. Ocean tomography is based on receiving a signal from a source with precisely known origin and inferring temperature. As with the *San Juan* signal, arrival times depend explicitly on the depth and range dependence of the ocean temperature. Modal arrivals comprising the dispersed signal propagate through different depth regimens (e.g., refer to the polar profile propagation in **Figure 6**, ***right***) and each provides an additional depth-dependent constraint to estimate the ocean climatic state. Acoustic thermometry (tomography) was proven viable through experiments starting as early as the 1970s (Spindel and Worcester, 2016) and began to be implemented from 1997 to 2006 during the Acoustic Thermometry for Ocean Climate program (Worcester et al., 2005). Now, with the six CTBT hydroacoustic stations online, there is a "cost-free" (expense absorbed by its primary mission) set of receivers and data repositories with which to implement these studies.

Summary

The CTBT hydroacoustic stations proved invaluable to the discovery of the *San Juan* submarine. **Figure 9** shows the map of the data used to plan the search (***red star*** is "the 'as found' position, only 8 nm [15 km] from the US and CTBTO centroids"; Ocean Infinity, personal communication, 2019). This amazing feat, pinpointing the location of a source to

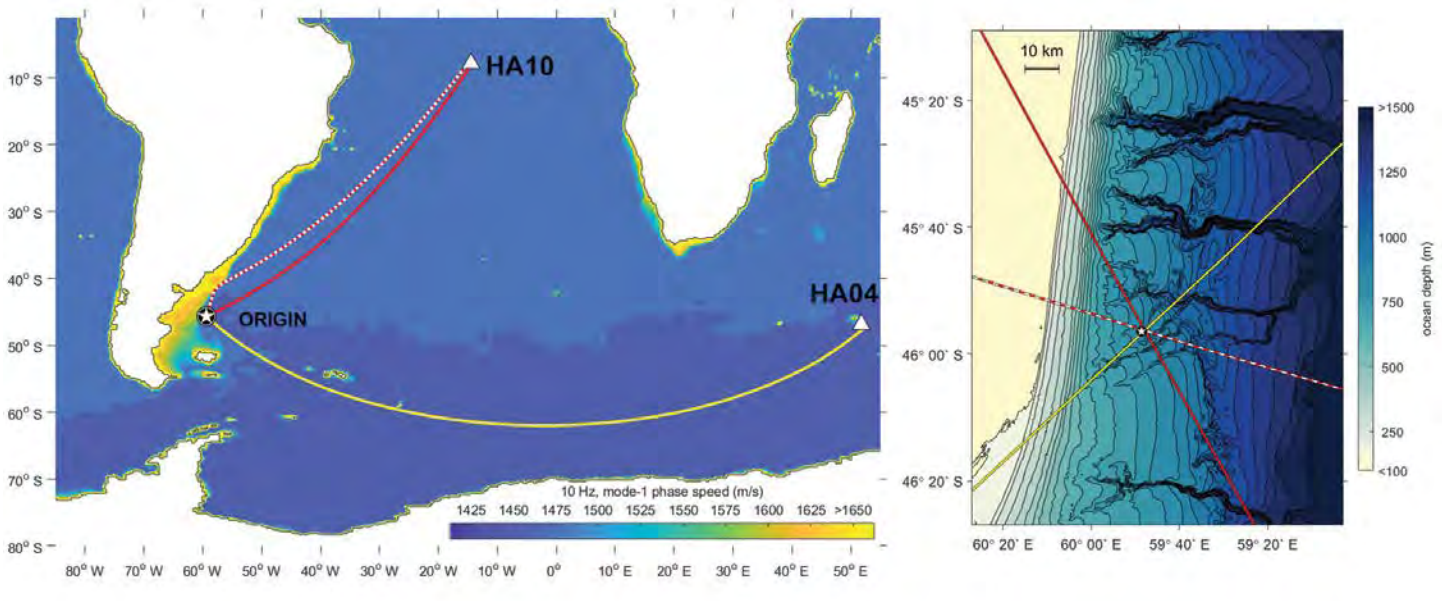

Figure 8. Left: *three mode-1 arrivals to triangulate the ARA* San Juan *(**star**), plotted over a map of its phase speed at 10 Hz. **Right**: intersection of the corresponding "isochrons" plotted over the bathymetry.*

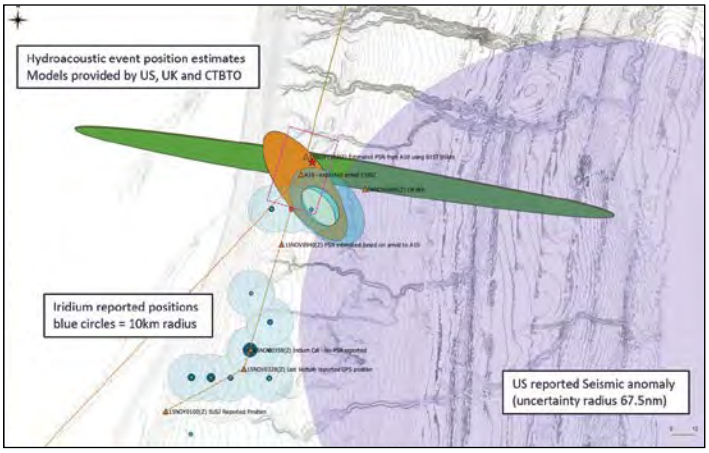

Figure 9. *Search map showing data from Iridium telecommunication satellite fixes (**blue circles**) and various modeled locations based on the recorded impulse. A combination of seismic and hydroacoustic detections were used and predicted the ARA* San Juan *location (**red star**) to within 8 nautical miles. Image provided by Ocean Infinity.*

within 1/1,000 of the propagation distance, was possible because the IMS network requires such precision to accomplish its mission, i.e., detecting and triangulating a nuclear explosion within an area no larger than 1,000 km^2 (Protocol to the CTBT, Part IIA). Triangulation of an unknown source requires at least three arrivals (the third arrival used in the triangulation was reported by the CTBTO in 2017; see **Figure 9**) was on a land-based seismic station. A pure hydroacoustic triangulation of the *San Juan* is possible if 3-D paths are considered. With the location of the *San Juan* now known, it is a dataset to baseline alternative methods of locating such signals of unknown origin.

Ultimately, error in triangulation depends on how well the actual ocean climate is characterized. Although yet to be implemented in any systematic way, the real-time data collection of the IMS network makes it possible to deploy a source and rapidly assess climatic anomalies such as those fueling the powerful thermal engine of a destructive hurricane. In fact, an example of this rapid assessment came two weeks after the *San Juan* went missing; an impulsive source (depth charge) was deployed to confirm the propagation characteristics. Beyond the critical mission of the IMS network (detections of nuclear explosions), the data it has collected and continues to collect can be used for other important purposes. Tsunami detection and enhanced early warning and geolocation of lost submarines, ships, and planes as well as assessments of cetacean populations and other marine life all can be derived from analyzing IMS data. The possibilities for the productive use of the historical and real-time IMS data are limitless.

References

Bradley, D. L., and Nichols, S. M. (2015). Worldwide low-frequency ambient noise. *Acoustics Today* 11(1), 20-26. https://doi.org/10.1121/AT.2015.11.1.20.

Bureau of Naval Personnel. (1953) *Naval Sonar*. NAVPERS 10884, US Government Printing Office, Washington, DC.

Dall'Osto, D. R. (2019). Source triangulation utilizing three-dimensional arrivals: Application to the search for the ARA San Juan submarine. *The Journal of the Acoustical Society of America* 146(3), 2104-2112.

Frisk, G. V. (1994). *Ocean and Seabed Acoustics*. Prentice Hall, Edgewood Cliffs, NJ.

Munk, W. H., and Zachariasen, F. (1991). Refraction of sound by islands and seamounts. *Journal of Atmospheric Oceanic Technology* 8, 554-574.

National Research Council. (2011). *National Security Implications of Climate Change for U.S. Naval Forces. Chapter 5: Climate-Change-Related Technical Issues Impacting U.S. Naval Operations.* The National Academies Press, Washington, DC.

Sabra, K. G., Cornuelle, B., and Kuperman, W. A. (2016). Sensing deep-ocean temperatures. *Physics Today* 69(2), 32-38.

Spindel, R. C., and Worcester, P. F. (2016). Walter H. Munk: Seventy-five years of exploring the seas. *Acoustics Today* 12(1), 36-42. https://doi.org/10.1121/AT.2016.12.1.36.

Villán, J. L. (2019). The tragic loss of ARA S*an Juan*. *Proceedings of the U.S. Naval Institute* 45, 1393.

Worcester, P. F., Munk, W. H., and Spindel, R. C. (2005). Acoustic remote sensing of ocean gyres. *Acoustics Today* 1(1), 11-17. https://doi.org/10.1121/1.2961121.

BioSketch

David R. Dall'Osto received his PhD in mechanical engineering from the University of Washington (Seattle) in 2013. Currently, he is a senior research scientist and engineer at the Applied Physics Laboratory, University of Washington. His research focus includes modeling and measurement of acoustic vector intensity in the ocean and atmosphere on both short-range and global scales. His work with the Comprehensive Nuclear Test Ban Treaty (CTBT) data originates from a detective role, and he has found great satisfaction in applying forensic acoustics to resolve ocean mysteries.